POLITECNICO DI TORINO
Repository ISTITUZIONALE

Digital Fairness in Satellite IoT Systems Based on NOMA With Nonideal SIC

Original
Digital Fairness in Satellite IoT Systems Based on NOMA With Nonideal SIC / Taricco, G.. - In: IEEE INTERNET OF THINGS JOURNAL. - ISSN 2327-4662. - 12:24(2025), pp. 55945-55948. [10.1109/jiot.2025.3618974]

Availability:
This version is available at: 11583/3006178 since: 2026-03-20T19:45:26Z

Publisher:
IEEE

Published
DOI:10.1109/jiot.2025.3618974

Terms of use:

This article is made available under terms and conditions as specified in the corresponding bibliographic description in the repository

Publisher copyright
IEEE postprint/Author's Accepted Manuscript

©2025 IEEE. Personal use of this material is permitted. Permission from IEEE must be obtained for all other uses, in any current or future media, including reprinting/republishing this material for advertising or promotional purposes, creating new collecting works, for resale or lists, or reuse of any copyrighted component of this work in other works.

(Article begins on next page)

09 November 2026

Digital Fairness in Satellite IoT Systems Based on NOMA with Nonideal SIC

Giorgio Taricco *Fellow, IEEE*†

***Abstract*—Achieving digital fairness through NOMA is a critical challenge in modern 5G/6G wireless systems, particularly for satellite uplinks supporting IoT devices across wide coverage areas. The variation in link budgets across space and time increases the risk of unequal access, allowing only a subset of users to achieve sufficiently high transmission rates. This work examines a coordinated uplink NOMA systems to equalize IoT user rates. It also incorporates the impact of imperfect SIC to reflect practical scenarios. For single-slot NOMA, the optimal SIC ordering to maximize the minimum user rate is determined. For multi-slot NOMA, relevant to satellite scenarios, a user rate equalization algorithm is proposed and analyzed numerically, assessing the trade-off between user rates and receiver complexity. The proposed algorithm addresses multi-slot scheduling constraints with SIC limitations—a critical aspect of fairness in practical systems—by leveraging temporal dynamics to achieve fair resource allocation.**

***Index Terms*—5G, 6G, Uplink NOMA, Successive Interference Cancellation (SIC), LEO satellite IoT networks, Digital fairness.**

I. Introduction

Non-Orthogonal Multiple Access (NOMA) is a key technique for 5G and beyond, enabling multiple users to share time-frequency resources and improving spectral efficiency over OMA. In uplink systems, varying channel conditions and power levels raise fairness challenges. MAX-MIN fairness, which maximizes the minimum achievable rate, has been widely studied as a fairness criterion in this context. For example, Zhang *et al.* [1] explored MAX-MIN fairness for uplink NOMA systems under finite blocklength constraints. Xu and Clerckx [2] proposed an uplink MIMO RSMA framework for short-packet communications with perfect channel state information. Liu *et al.* [3] address the near-far problem in wireless-powered communication networks using a fairness-aware NOMA-based scheduling scheme to enhance max-min fairness. Focusing on uplink NOMA satellite communication systems, it has been observed that achieving fairness among users with diverse channel conditions, transmission powers, and geometrical positions poses unique challenges. The inherent differences in user distances from the satellite, combined with non-uniform beamforming gains and frequency reuse patterns, exacerbate the disparity in signal quality, making resource allocation and interference management critical to ensuring equitable access to communication services. Additionally, the high mobility of satellites in low Earth orbit (LEO) introduces dynamic changes in user-satellite geometry, necessitating adaptive algorithms to maintain fairness and quality-of-service guarantees in real-time.

The integration of NOMA in uplink satellite and related IoT communication scenarios has been extensively studied to address challenges like fairness, spectral efficiency, and dynamic user associations. In this area, Wang *et al.* [4] proposed a NOMA-enabled framework for multi-beam satellite systems to overcome the mismatch between offered capacity and requested traffic. From a different standpoint, Ahsan *et al.* [5] explored the use of reinforcement learning in uplink NOMA for Internet of Things (IoT) networks. In a related context, Nauman *et al.* [6] examined a vehicular-aided heterogeneous network (HetNet) with High Altitude Platforms (HAPs) and uplink NOMA. In the framework of MAX-MIN fairness for uplink NOMA, Gao *et al.* [7] provide evidence that the optimum SIC order corresponds to decoding the signals from the stronger to the weaker but with the goal of minimizing an outage probability, which is not equivalent to the case considered here. Finally, to enhance the practical relevance of this study, the analysis incorporates the effects of imperfect SIC, as discussed in previous works [8], [9]. Its impact on the rate performance is captured, providing a more realistic evaluation of how deviations from the perfect SIC assumption may affect the system.

Moreover, practical wireless systems are affected by hardware impairments such as power amplifier nonlinearities, oscillator phase noise, and in-phase/quadrature (I/Q) imbalance, which can degrade the signal quality and significantly impact the performance of uplink NOMA systems if not properly accounted for [10], [11].

Contributions. After presenting a realistic coordinated uplink satellite IoT scenario, we optimize a NOMA scheme with imperfect SIC for single- and multi-slot cases. In the single-slot case, Proposition 1 shows that the MAX-MIN achievable rate is attained with a nonincreasing SNR sequence, even with imperfect SIC. In the multi-slot case, Algorithm 1 effectively equalizes user rates by considering each user's cumulative reward rather than using a simple round-robin approach. Numerical results demonstrate the throughput performance and compare it with standard OMA.

II. Satellite beamspot scenario

The scenario is inspired by the Starlink network [12]–[14], with simplifying assumptions. Starlink satellites orbit in multiple shells with nearly circular paths and a 90-minute period, yielding an angular speed of $0.067^\circ/\text{s}$. The typical

† Giorgio Taricco is with Politecnico di Torino, Italy. Copyright (c) 20xx IEEE. Personal use of this material is permitted. However, permission to use this material for any other purposes must be obtained from the IEEE by sending a request to pubs-permissions@ieee.org.

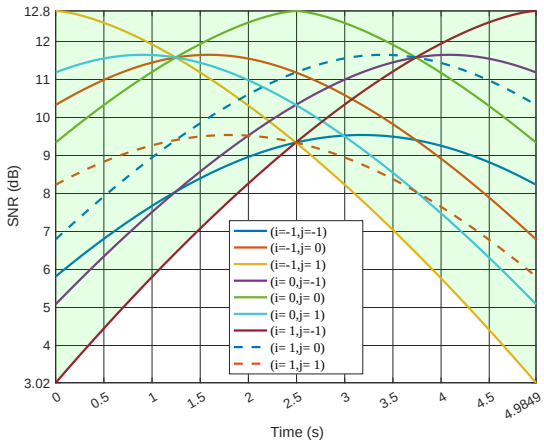

Fig. 1. SNR diagrams corresponding to user locations $(\lambda_0+i\delta_{\mathsf{lat}}, \varphi_0+j\delta_{\mathsf{lon}})$ for $i,j \in \{-1,0,1\}$ in latitude/longitude coordinates. The light green area corresponds to the SNR range over the coverage area.

3-dB antenna beamwidth is $3.5°$, corresponding to a central Earth angle of $0.3°$ and a satellite passage time of about 4.5 s. We consider a scenario where the satellite orbits at 550 km from the Earth surface and transmits in the Ku-band at 14 GHz. The satellite antenna is pointed to the nadir with maximum gain $G_{\mathsf{max}} = 36$ dBi. The IoT terminals transmit at a power of $P_{\mathsf{tx}} = 10$ W, with antenna gain of 3 dBi. Free-space path loss is used for signal attenuation, based on the distance between the satellite and the IoT terminals. A line-of-sight (LOS) model is used, assuming no obstructions or atmospheric effects (*clear-sky* conditions). The received signal power from each IoT terminal is calculated by the Friis equation [15]:

$$P_{\mathsf{rx}} = G_{\mathsf{term}} G_{\mathsf{sat}}(\psi) \left(\frac{\lambda}{4\pi d}\right)^2 P_{\mathsf{tx}} \tag{1}$$

P_{tx} is the transmitted power from the IoT terminal, G_{term} is the IoT terminal's antenna gain (0 dBi for an isotropic antenna), $G_{\mathsf{sat}}(\psi)$ is the satellite antenna gain, modeled according to [16, recomm. 1.2] with $\alpha = 1.5$, ψ is the off-axis angle, λ is the carrier wavelength, and d is the propagation distance. The received SNR is:

$$\mathsf{SNR} = \frac{P_{\mathsf{rx}}}{P_{\mathsf{noise}}} = \frac{P_{\mathsf{rx}}}{kT_0B}, \tag{2}$$

with $k = 1.38 \cdot 10^{-23}$ J/K, Boltzmann constant, $T_0 = 290$ K, and $B = 10$ MHz is the system bandwidth. The coverage region is defined by the latitude/longitude ranges:

$$\lambda \in (\lambda_0 - \delta_{\mathsf{lat}}, \lambda_0 + \delta_{\mathsf{lat}}), \quad \varphi \in (\varphi_0 - \delta_{\mathsf{lon}}, \varphi_0 + \delta_{\mathsf{lon}})$$

with $\delta_{\mathsf{lat}} = 0.1°$ and $\delta_{\mathsf{lon}} = 0.1 \cdot \tan(53°) = 0.133°$. The satellite nadir passes through the center of the region (λ_0, φ_0) with an inclination of $53°$ with respect to the equatorial plane, and the passage time is $\frac{0.2°}{\cos(53°)\cdot 0.067°/\mathrm{s}} = 4.98$ s. The received SNR corresponding to the nine user locations characterized by their latitude/longitude coordinates $(\lambda_0 + i\delta_{\mathsf{lat}}, \varphi_0 + j\delta_{\mathsf{lon}})$ for $i,j \in \{-1,0,1\}$ is illustrated in Fig. 1. The scenario is further detailed by including a total of N users within the coverage area and dividing the time frame into T time slots, during which the received SNRs remain nearly constant (*e.g.*, setting $T = 100$ limits the SNR variability within each slot to approximately 0.1 dB or less).

III. Uplink IoT NOMA

Consider a coordinated multiuser communication system where N IoT user terminals transmit to a LEO satellite by using a NOMA technique. The terminals, labeled by $n = 1, \ldots, N$, transmit over a sequence of T time slots labeled by $t = 1, \ldots, T$. The channel gain is (approximately) constant over the time slots so that the received signal at the satellite is:

$$Y[t] = \sum_{n=1}^{N} H_n[t] X_n[t] + Z_n[t], \quad t = 1, \ldots, T. \tag{3}$$

Define the satellite receiver SNRs:

$$\rho_n[t] \triangleq \frac{|H_n[t]|^2 P_n[t]}{P_z}, \tag{4}$$

where $P_n[t]$ is the average transmitted power from the n-th IoT user terminal during the t-th time slot and P_z is the average receiver noise power. Following the Superposition Encoding and Successive Interference Cancellation (SIC) approach (see, *e.g.*, [17]), the achievable rates of the multiple-access multiuser communication system are given by:

$$R_n[t] = \log_2\left(1 + \frac{\rho_n[t]}{1 + \phi \sum_{m<n} \rho_m[t] + \sum_{m>n} \rho_m[t]}\right) \tag{5}$$

for $n = 1, \ldots, N$ and $t = 1, \ldots, T$. Here, the coefficient $\phi \in [0,1]$ accounts for the presence of residual interference after SIC (see, *e.g.*, [8], [9]). The rate $R_n[t]$ is achieved by decoding the codeword corresponding to user n during the time slot t after decoding the codewords corresponding to the users $1, \ldots, n-1$ and, after each decoding, re-encoding the information symbols and removing their contribution from the received signal. It is plain that, with *ideal SIC* ($\phi = 0$),

$$R_{\mathrm{sum}}[t] = \sum_{n=1}^{N} R_n[t] = \log_2(1 + \rho_1[t] + \ldots + \rho_N[t]) \tag{6}$$

is achieved. In order to minimize the spreading of the achievable rates when $\phi > 0$, interference cancellation proceeds from the strongest to the weakest user:

Proposition 1: For a given set of SNRs, $\{\rho_1, \ldots, \rho_N\}$, the MAX-MIN achievable rate is obtained when the SNR sequence is nonincreasing.

In the ideal SIC case, this is referred to as *natural order* for an uplink multiuser channel in [17, Sec. 6].

Proof: See App. A. ■

A. Multi-slot optimization

This section considers the achievability of digital fairness over a longer time span covering multiple time slots. Considering N IoT user terminals accessing a NOMA uplink with a maximum power P_{tx}, we define a *feasible power region*

$$\mathcal{P} \triangleq \{P_n[t] \le P_{\mathsf{tx}}, n = 1, \ldots, N, t = 1, \ldots, T\}. \tag{7}$$

Since the IoT user terminals aim to exploit the achievable information rate to the satellite during its passage on the

coverage area, the following optimization problem based on a MAX-MIN fairness criterion can be formulated:

$$\max_{P_n[t]\in\mathcal{P}} \min_{1\le n\le N} \bar{R}_n[T], \tag{8}$$

where $R_n[t]$ is the rate given by (5) and $\bar{R}_n[t] \triangleq \sum_{\tau=1}^{t} R_n[\tau]$ is the cumulative rate. During each time-slot, the cancellation order at the receiver and the transmission powers are chosen according to Prop. 1. Complexity limitations related to the implementation of SIC suggest to limit the transmitting users per time slot to a maximum number, N_{SIC} [1]. Algorithm 1 optimizes the multi-slot performance based on these results with a complexity $O((N + N_{\mathsf{SIC}}) \log N_{\mathsf{SIC}})$.

Algorithm 1 Uplink NOMA multi-slot optimization

Input: $\rho_n[t], n = 1, \ldots, N, t = 1, \ldots, T$ and N_{SIC}
Output: $\tilde{\rho}_n[t], n = 1, \ldots, N, t = 1, \ldots, T$
Initialize the cumulative rates $\bar{R}_n[0] = 0, n = 1, \ldots, N$
for $t = 1, \ldots, T$ **do**
    Select the N_{SIC} users with minimum $\bar{R}_n[t]$
    Let $\mathcal{N}_{\mathsf{SIC}}[t]$ denote this set of users
    Apply Prop. 1 to calculate the rates $R_n[t]$
    for all $n \in \mathcal{N}_{\mathsf{SIC}}[t]$
    Update the cumulative rates $\bar{R}_n[t] = \bar{R}_n[t-1] + R_n[t]$
    for all $n \in \mathcal{N}_{\mathsf{SIC}}[t]$
end for
return $\mathcal{N}_{\mathsf{SIC}}[t], \tilde{\rho}_n[t], \bar{R}_n[t]\ \forall\ n = 1, \ldots, N, t = 1, \ldots, T$

B. OMA

The results obtained by using NOMA are compared with Orthogonal Multiple Access (OMA), where the achievable rates are:

$$R_n^{\mathsf{OMA}}[t] = \frac{\log_2(1 + \rho_n[t])}{|\mathcal{N}[t]|}, \tag{9}$$

where $\mathcal{N}[t]$ is the set of active users at time t. Multi-slot optimization can be implemented as in the case of NOMA considered in Algorithm 1 after replacing $\mathcal{N}_{\mathsf{SIC}}[t]$ by $\mathcal{N}[t]$.

IV. Numerical Results

This section presents numerical results with $N = 256$ IoT user terminals uniformly distributed over a 16×16 square lattice over the coverage area. The satellite cycle time of about 5 seconds is partitioned into $T = 100$ time slots of 50 ms. Algorithm 1 is used to calculate the achievable rates for the bandwidth $B = 10$ MHz, using a periodic extension of the satellite cycle time over a sufficiently large number of repetitions ($N_{\mathsf{rep}} = 100$). Figs. 3 and 2 illustrate the user achievable rates for $\nu = N_{\mathsf{SIC}} = 2^p, p \in [0, 7] \cap \mathbb{Z}$ and $\phi = 0$ (ideal SIC) and 0.01, respectively.[2] The figure also includes: i) the corresponding OMA rates obtained by enabling ν users per symbol time (as with NOMA) and ii) the average sum-rate across the $N_{\mathsf{rep}}T$ time slots. The caption reports the standard deviations σ of the user achievable rates. This measures the *user fairness* achieved by Algorithm 1. Fig. 4 shows the time behavior of the minimum sum rate divided by the current time, i.e., $\min_{1\le n\le N} \bar{R}_n[t]/t$. The curves illustrate the convergence speed of Algorithm 1. Scalability is maintained up to $N \approx 10^4$ users (the other parameters being kept fixed).

[1] The other users must not be transmitting during the time slot. This requires network coordination and is incompatible with grant-free transmission [18].

[2] $\phi = 0.01$ corresponds to the worst case considered in [9].

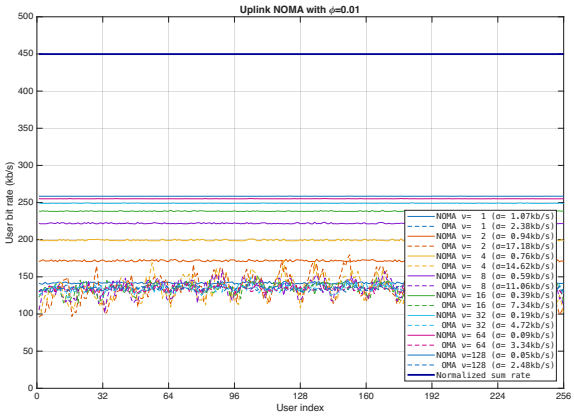

Fig. 2. User achievable rates obtained by applying Algorithm 1 to the scenario considered with perfect SIC. The upper limit labeled "Normalized sum-rate" corresponds to $\frac{1}{T}\sum_t \log_2(1 + \sum_n \rho_n[t]) \cdot B$.

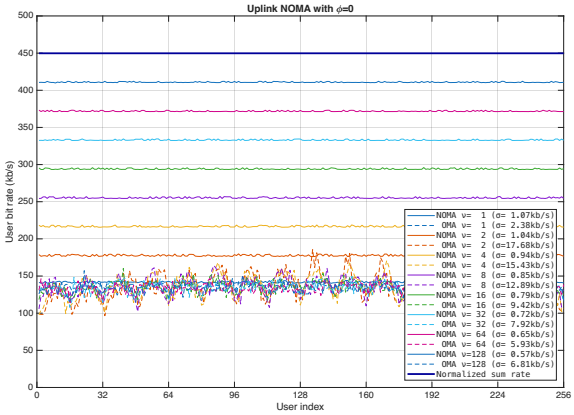

Fig. 3. Same as Fig. 2 but $\phi = 0$ (ideal SIC).

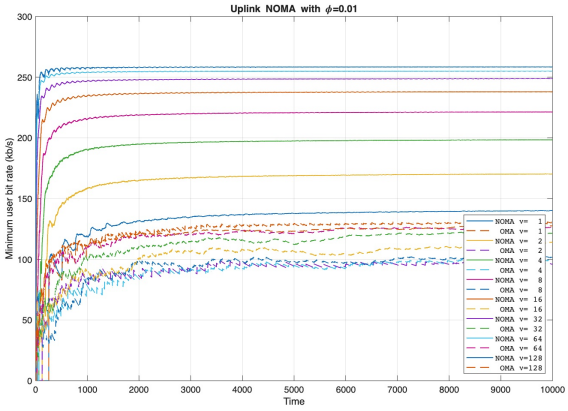

Fig. 4. Plot of the minimum cumulative rate with $\phi = 0.01$.

V. Conclusions

Digital fairness in Non-Orthogonal Multiple Access (NOMA) systems is a critical challenge, particularly in 5G/6G satellite uplinks where IoT devices face variable link budgets. This variability often limits some users from transmitting effectively, creating inequities in network performance. For single-slot NOMA, the optimal cancellation order at the receiver has been derived. In multi-slot NOMA, a novel algorithm for digital fairness has been proposed and analyzed with ideal and imperfect SIC represented by the factor ϕ, which provides a practical means of quantifying this degradation. These results offer practical guidance for satellite IoT operators, showing that the proposed algorithms can be integrated into existing LEO scheduling protocols to optimize throughput and resource utilization, reduce latency in time-sensitive communications, and enable adaptive allocation of network resources based on dynamic traffic loads and link availability, thereby enhancing overall network performance and reliability.

Appendix A
Proof of Proposition 1

Consider switching the values of ρ_a and ρ_b with $a < b$ and $\rho_a < \rho_b$ and let R_i' be the rate after the switch. Assume $\phi < 1$. We need to show that, in all cases, $\min_i R_i \leq \min_i R_i'$. It is plain to see that, if $a < b < i$ or $i < a < b$, $R_i' = R_i$, so that we need to consider only the case $a \leq i \leq b$. If $a < i < b$, $R_i < R_i'$ since

$$R_i = \log_2\left(1 + \frac{\rho_i}{1 + \phi\sum_{j<i}\rho_j + \sum_{j>i}\rho_j}\right) \text{ and } R_i' = \log_2\left(1 + \frac{\rho_i}{1 + \phi\sum_{j<i}\rho_j + \sum_{j>i}\rho_j - (1-\phi)(\rho_b - \rho_a)}\right)$$

If $i = a$,

$$R_a = \log_2\left(1 + \frac{\rho_a}{1 + \phi\sum_{j<a}\rho_j + \sum_{j>a}\rho_j}\right),$$
$$R_a' = \log_2\left(1 + \frac{\rho_b}{1 + \phi\sum_{j<a}\rho_j + \sum_{j>a}\rho_j - (\rho_b - \rho_a)}\right).$$

If $i = b$,

$$R_b = \log_2\left(1 + \frac{\rho_b}{1 + \phi\sum_{j<b}\rho_j + \sum_{j>b}\rho_j}\right),$$
$$R_b' = \log_2\left(1 + \frac{\rho_a}{1 + \phi\sum_{j<b}\rho_j + \sum_{j>b}\rho_j + \phi(\rho_b - \rho_a)}\right).$$

Then, denoting the denominators in the expressions of R_a, R_a', R_b', as D_a, D_a', D_b', respectively, we get:

$$D_a - D_a' = \rho[b] - \rho[a] > 0, D_a - D_b' = (1-\phi)\sum_{j=a+1}^{b}\rho_j > 0.$$

These inequalities and $\rho[a] < \rho[b]$ imply that $R_a < R_a'$ and $R_a < R_b'$. Therefore, $\min\{R_a, R_b\} < \min\{R_a', R_b'\}$. This inequality and the fact that $R_i < R_i'$ complete the proof. ■

References

[1] Y. Zhang, T. Zhong, Y. Wang, J. Wang, K. Zheng, and X. You, "Max-Min fairness for uplink NOMA systems with finite blocklength," *IEEE Transactions on Vehicular Technology*, vol. 73, no. 3, pp. 4447–4452, March 2024.

[2] J. Xu and B. Clerckx, "Max-min fairness and PHY-layer design of uplink MIMO rate-splitting multiple access with finite blocklength," *IEEE Transactions on Communications*, pp. 1–1, 2024.

[3] Y. Liu, X. Chen, L. X. Cai, Q. Chen, R. Gong, and D. Tang, "On the fairness performance of NOMA-based wireless powered communication networks," in *ICC 2019 - 2019 IEEE International Conference on Communications (ICC)*, May 2019, pp. 1–6.

[4] A. Wang, L. Lei, E. Lagunas, A. I. Pérez-Neira, S. Chatzinotas, and B. Ottersten, "NOMA-enabled multi-beam satellite systems: Joint optimization to overcome offered-requested data mismatches," *IEEE Transactions on Vehicular Technology*, vol. 70, no. 1, pp. 900–913, Jan 2021.

[5] W. Ahsan, W. Yi, Z. Qin, Y. Liu, and A. Nallanathan, "Resource allocation in uplink NOMA-IoT networks: A reinforcement-learning approach," *IEEE Transactions on Wireless Communications*, vol. 20, no. 8, pp. 5083–5098, Aug 2021.

[6] A. Nauman, M. Maashi, H. K. Alkahtani, F. N. Al-Wesabi, N. O. Aljehane, M. Assiri, S. S. Ibrahim, and W. U. Khan, "Efficient resource allocation and user association in NOMA-enabled vehicular-aided HetNets with high altitude platforms," *Computer Communications*, vol. 216, pp. 374–386, 2024.

[7] Y. Gao, B. Xia, K. Xiao, Z. Chen, X. Li, and S. Zhang, "Theoretical analysis of the dynamic decode ordering SIC receiver for uplink NOMA systems," *IEEE Communications Letters*, vol. 21, no. 10, pp. 2246–2249, Oct 2017.

[8] Z. Wei, D. W. K. Ng, J. Yuan, and H.-M. Wang, "Optimal resource allocation for power-efficient MC-NOMA with imperfect channel state information," *IEEE Transactions on Communications*, vol. 65, no. 9, pp. 3944–3961, Sep. 2017.

[9] S. Wang, T. Lv, W. Ni, N. C. Beaulieu, and Y. J. Guo, "Joint resource management for MC-NOMA: A deep reinforcement learning approach," *IEEE Transactions on Wireless Communications*, vol. 20, no. 9, pp. 5672–5688, 2021.

[10] X. Zhang, M. Matthaiou, E. Björnson, M. Coldrey, and M. Debbah, "On the mimo capacity with residual transceiver hardware impairments," in *2014 IEEE International Conference on Communications (ICC)*, June 2014, pp. 5299–5305.

[11] E. Björnson, J. Hoydis, M. Kountouris, and M. Debbah, "Massive mimo systems with non-ideal hardware: Energy efficiency, estimation, and capacity limits," *IEEE Transactions on Information Theory*, vol. 60, no. 11, pp. 7112–7139, Nov 2014.

[12] F. Rinaldi, H.-L. Maattanen, J. Torsner, S. Pizzi, S. Andreev, A. Iera, Y. Koucheryavy, and G. Araniti, "Non-terrestrial networks in 5G & beyond: A survey," *IEEE Access*, vol. 8, pp. 165 178–165 200, 2020.

[13] M. M. Azari, S. Solanki, S. Chatzinotas, O. Kodheli, H. Sallouha, A. Colpaert, J. F. Mendoza Montoya, S. Pollin, A. Haqiqatnejad, A. Mostaani, E. Lagunas, and B. Ottersten, "Evolution of non-terrestrial networks from 5G to 6G: A survey," *IEEE Communications Surveys & Tutorials*, vol. 24, no. 4, pp. 2633–2672, Fourthquarter 2022.

[14] G. Maiolini Capez, M. A. Cáceres, R. Armellin, C. P. Bridges, J. A. Fraire, S. Frey, and R. Garello, "On the use of mega constellation services in space: Integrating LEO platforms into 6G non-terrestrial networks," *IEEE Journal on Selected Areas in Communications*, vol. 42, no. 12, pp. 3490–3504, Dec 2024.

[15] C. A. Balanis, *Antenna Theory: Analysis and Design*, 4th ed. John Wiley & Sons, 2016.

[16] International Telecommunication Union, "Satellite antenna radiation patterns for non-geostationary orbit satellite antennas operating in the fixed-satellite service below 30 GHz," International Telecommunication Union, Tech. Rep. ITU-R S.1528, 2001.

[17] D. Tse and P. Viswanath, *Fundamentals of Wireless Communication*, ser. Wiley series in telecommunications. Cambridge University Press, 2005.

[18] M. B. Shahab, R. Abbas, M. Shirvanimoghaddam, and S. J. Johnson, "Grant-free non-orthogonal multiple access for IoT: A survey," *IEEE Communications Surveys & Tutorials*, vol. 22, no. 3, pp. 1805–1838, third quarter 2020.